Ecological Indicators 157 (2023) 111281

Contents lists available at ScienceDirect

Ecological Indicators

journal homepage: www.elsevier.com/locate/ecolind

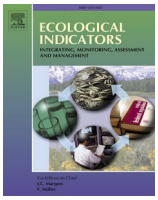

Airborne laser scanning to optimize the sampling efficiency of a forest management inventory in South-Eastern Germany

Tristan R.H. Goodbody [a,*], Nicholas C. Coops [a], Cornelius Senf [b], Rupert Seidl [b,c]

[a] Faculty of Forestry, University of British Columbia 2424 Main Mall, Vancouver, British Columbia V6T 1Z4, Canada
[b] Department of Life Science Systems, TUM School of Life Sciences, Technical University of Munich, Hans-Carl-von-Carlowitz-Platz 2, Freising 85354, Germany
[c] Berchtesgaden National Park, Doktorberg 6, Berchtesgaden 83471, Germany

ARTICLE INFO

Keywords:
Forest structure
Airborne laser scanning
LiDAR
Optimization
Sampling

ABSTRACT

Effective forest stewardship relies on comprehensive field-inventories describing forest resources. Increasing demands for data and indicators that improve understanding of climate change impacts, timber production, and ecosystem processes make access to robust field inventories crucial. A trade-off between cost and statistical efficacy exists however, necessitating that practitioners be familiar with the spatial and structural composition and variability of their management areas. Remotely sensed data, like airborne laser scanning (ALS), can improve data availability and sampling efficiency. In this study, we simulate sampling approaches and provide an indication of the benefits of incorporating ALS-derived auxiliary data. We evaluate the ability of sub-samples from an existing field-inventory to accurately estimate ALS structural metrics. Additionally, we explore data-driven approaches to allocate new field plots, reducing bias and improving accuracy. The Monte Carlo simulation compared the local pivotal method (LPM), Latin hypercube sampling (LHS), and simple random sampling (SRS) at a variety of sample sizes. Precision and variability measures were used to comparatively assess the efficacy of sampling method and sample size. Results demonstrate the value of ALS as an auxiliary dataset, with LPM and LHS achieving sampling efficiencies over SRS of up to 88.6% and 94.3%, respectively. By applying the adapted Latin hypercube evaluation of a legacy sample (AHELS) algorithm, we reduced the mean average percent deviation (MAPD) by over 20% between sample measures and wall-to-wall ALS metrics. These methods can aid practitioners in planning cost-effective and statistically rigorous forest inventory campaigns, particularly in determining where to re-sample within an existing plot network.

1. Introduction

Forests are increasingly considered to be critical global resources for their roles in climate change mitigation strategies (Canadell & Raupach, 2008), the growing bioeconomy (Verkerk, 2022), and transition towards models of sustainable growth and development (Kurniawan & Managi, 2018; Swamy et al., 2018). It is imperative therefore to have accurate and up-to-date data and knowledge on the state and composition of forest resources, but this task is anything but trivial. Forests are highly dynamic ecosystems in a constant state of change resulting from vegetation growth, but also biotic (e.g. insect and fungal infections) and abiotic disturbances (e.g. windthrow, wildfire, harvest) that impact their spatial and structural compositions (Senf et al., 2017). Our traditionally timber-focused paradigm towards forest resources is steadily shifting to incorporate more holistic ecosystem-based management approaches, where more indicators for forest heterogeneity are a requirement. Current and future stewardship of forest resources in our rapidly changing world therefore hinges on the inventory methods we use and their ability to capture and integrate forest heterogeneity.

Enhanced forest inventories (EFI) integrate forestry ground plot measurements with remote sensing technologies – principally airborne laser scanning (ALS) – to produce spatially contiguous fine grain (20 – 30 m) modelled estimates of key attributes including height, biomass, and stem density amongst others. Use of EFIs continues to grow due to their accurate, fine spatial estimates and ability to be utilised in forest management processes with considerable budgetary efficiencies over purely field-based methods. Reviews by Kangas et al. (2018), Aricak et al. (2022) and White et al. (2016) outlined state-of-the-art uses of ALS data for forest management and engineering where wall-to-wall structural and terrain information provide tangible operational, tactical, and

* Corresponding author.
E-mail address: goodbody.t@gmail.com (T.R.H. Goodbody).

https://doi.org/10.1016/j.ecolind.2023.111281
Received 24 August 2023; Received in revised form 24 September 2023; Accepted 15 November 2023
Available online 21 November 2023

strategic benefits. The resulting characterizations of forest structure in an EFI context have resulted in a paradigm shift in the way we conceptualize vegetation structure in forest ecosystem science and management (Maltamo et al., 2021).

Common to the EFI methodology is the area-based approach (ABA). The ABA is used to generate predictions of target forest attributes (e.g. above ground biomass, stem density) based on spatially explicit statistical summaries (metrics) of ALS structure that are often separated into height, cover, and density related sub-groups (Maltamo et al., 2021). These are then related to key forest attributes and indicators measured at plots in the field. The ABA has become a standard method (White et al., 2016), having seen extensive research and operational implementation in a variety of forest types globally (e.g. Corona and Fattorini, 2008; Gobakken, Korhonen and Næsset, 2013; White et al., 2013; Næsset, 2015; Tompalski et al., 2015; Hawryło et al., 2017; Ayrey et al., 2019; Iqbal et al., 2019).

Two fundamental pre-requisites exist for use of field plots for ABA and EFI development. First, plots must be spatially co-occurring with ALS data to enable forest attribute modelling, and second, plots should be measured as close in time as possible to ALS acquisitions to reduce temporal mismatches between field-measured attributes and ALS structure (Tompalski et al., 2018). When planning an EFI, managers will need to consider where – and how – to sample the forest area. Operational inventories often use temporary plots to gather information on trees and forest stands that are relevant to operational goals (e.g. estimate biomass prior to harvesting). In some cases, a permanent network of plots may exist, which with scheduled re-measurement cycles are intended to provide both measurement of the current state of the forest resource but also allow estimates of forest dynamics such as changes in forest cover, species composition, and biomass (Tomppo et al., 2010). Measurement frequency (e.g. every 10 years) however can be problematic for management-oriented inventories, which require fine temporal scale information related to dynamics to optimize economic incentives – an area where technologies like ALS and optical remotely sensed data have great potential.

Field measurement campaigns are expensive, however, and mangers face trade-offs between cost and the desired precision of estimates needed for effective decision making (de Papa et al., 2020). For both temporary and permanent sample designs, the focus shifts to optimizing plot number such that statistical value is maximized and costs are minimized. White et al. (2017) emphasize that the sample size required for an ABA depends on a number of factors. First, the complexity of the forested environment and variability of forest structure, with highly complex landscapes requiring more samples than a relatively simple forest. Second, its important to consider sample size in the context of the intended forest attribute (e.g. biomass) modelling approach. Some modelling methods such as imputation (e.g. K-NN) are incapable of extrapolating estimates, raising the importance of sampling designs that are spatially and empirically representative of the underlying population (Grafström et al., 2014). Third – and related to modelling – is the desired precision of estimates. Greater sample sizes will improve precision, but also increase costs. In this regard, research and toolkits focused on methods and technology transfer initiatives to optimize the balance between sample size and precision of the obtained estimates should be further explored (Goodbody et al., 2023).

Gobakken et al. (2013) found that ALS-assisted field plot selection resulted in predictive volume models with comparatively lower error to random plot locations, with independent validation data also revealing that ALS-assisted models resulted in smaller mean differences. Junttila et al. (2013) compared multiple systematic and random calibration plot selection methods, with findings that selection methods incorporating both spatial and feature space variability improved model performance. These findings are reinforced by Grafström and Ringvall (2013), Grafström et al. (2014), and Grafström and Lisic (2018), who presented approaches including the local pivotal method, an efficient strategy that ensures plots are well distributed in the environmental and geographic space spanned by auxiliary variables. Melville et al. (2015) found that relative efficiencies of two-fold or better were possible when using ALS data as *a priori* auxiliary information compared to random sampling. de Papa et al. (2020) used a simulated sampling approach to estimate the possible gains in field efficiencies based on ALS-aided stratifications. Their findings indicated that reductions in sample size of up to 41 % were possible relative to simple random sampling, which was noted to result in savings that offset ALS acquisition costs. Maltamo et al. (2021) stated that if *a priori* remotely sensed data are not used, and simple random or systematic sampling is performed, that there is a risk of not effectively capturing forest attribute variation. Overall, findings from these studies highlight the inherent value of ALS and remotely sensed data not only as predictors for forest attribute models, but also for *a priori* use in sample design and optimization. These benefits have prompted the creation of open-source software suites such as *sgsR* (Goodbody et al., 2023), which provide implementations for published methods of remote sensing-aided inventory design.

Of particular interest to forest practitioners that operate in areas with existing permanent plot networks is to understand which field plots to prioritize for remeasurement within the context of budgetary constraints. Complete remeasurement of an existing sample comprised of hundreds or even thousands of plots is unlikely unless long-term funding is secured. In these scenarios, practitioners need objective methods to optimize which field plots – and how many – to revisit to derive precise attribute estimates. Research outcomes outlining how to optimize which, and how many plots to remeasure are scarce and are worthy of exploration. To address this pertinent research need, in this study we explore the integration of wall-to-wall ALS metrics and an existing systematic sample. Using a Monte Carlo sampling simulation, we outline how leveraging *a priori* ALS metrics as auxiliary information can result in substantial sampling efficiencies. Through the comparison of three sampling methods (Latin hypercube sampling, local pivotal method, and simple random sampling) and incrementally increasing sample sizes, simulations are used to answer three questions.

1. Are sub-samples of an existing systematic plot network capable of precisely estimating parameters from the full sample, and if so, what degree of sampling efficiency can be realized?
2. Are resulting sub-samples capable of accurately estimating parameters from wall-to-wall ALS metrics?
3. Can data-driven methods for allocating new field plots be used to reduce any bias cost-effectively?

2. Materials and methods

2.1. Study area and inventory

The study area was the Berchtesgaden National Park (BGNP) situated in the northern front range of the Alps in South Eastern Germany (Fig. 1). BGNP is highly complex topographically with areas of steep and sheer slopes and elevations ranging from 603 to 2713 m above sea level. This study focuses exclusively on forested portions of the BGNP, which cover a total of 11,835 ha (tree line at approximately 1700 m asl) and has had an extensive history of forest management prior to its national park designation in 1978. The previous management history continues to influence contemporary vegetation structures and species compositions, which is primarily composed of coniferous stands dominated by Norway spruce (*Picea abies* (L.) Karst.) (54 %), followed by mixed stands (32 %) consisting mainly of Norway spruce, European beech (*Fagus sylvatica* L.), and silver fir (*Abies alba* Mill.), and stands dominated by European larch (*Larix decidua* L.) (12 %) and European beech (*Fagus sylvatica* L.) (2 %).

A sample-based forest inventory was established in BGNP in 1983 – 1985 on a systematic grid of 200×100 m. The inventory has been remeasured twice (1995 – 1997 & 2010–2012) and provides an important information base for park management (Becker, 2016) and

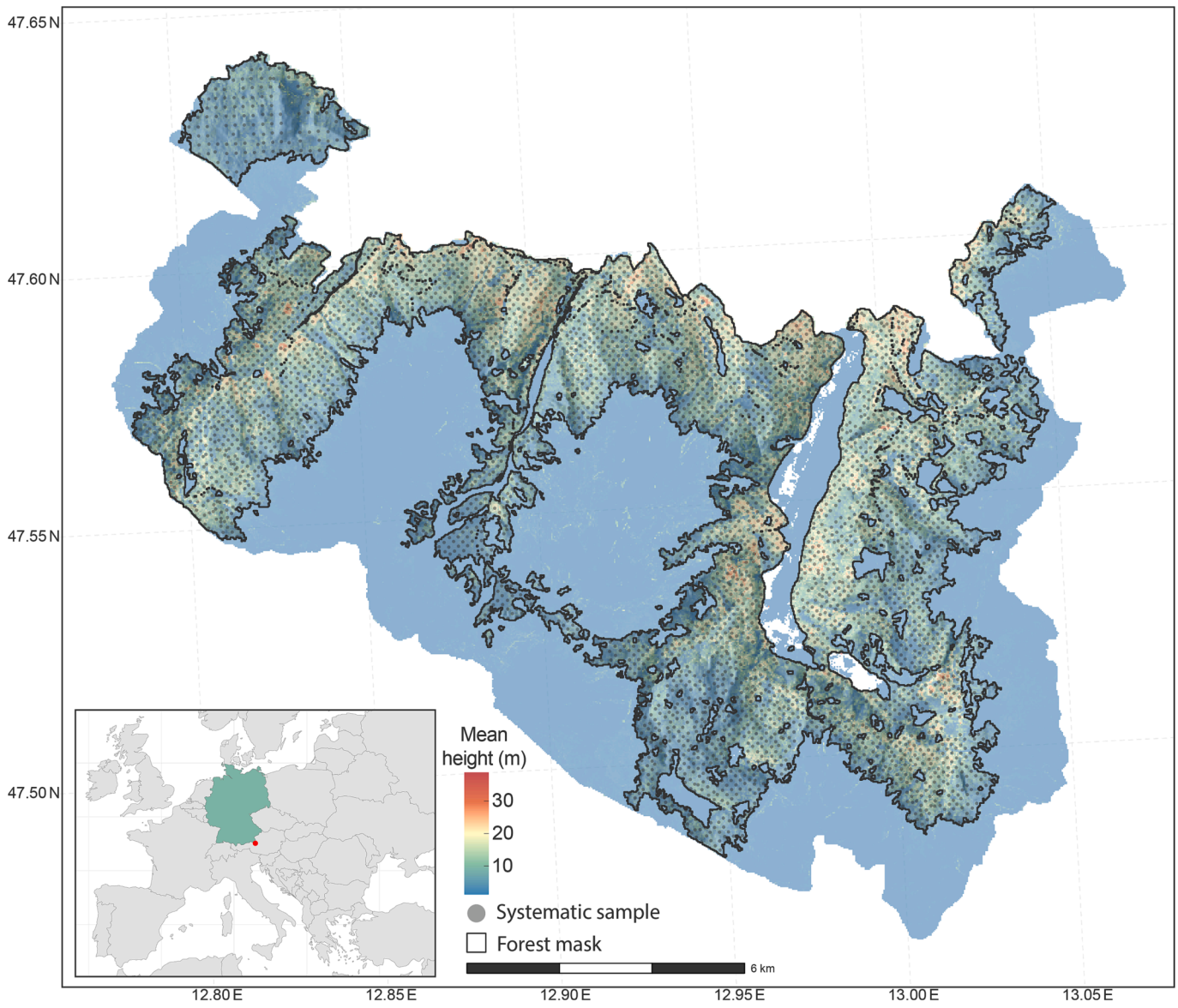

Fig. 1. Study area map of the Berchtesgaden National Park (BGNP) in Southeastern Germany with associated systematic sample (points), forest area mask (perimeter), and ALS-derived mean height (m).

scientific inquiry on ongoing forest change (Thom & Seidl, 2022). The first inventory included 5406 plots, which was extended to 5782 plots in the 2010 – 2012 inventory cycle to capture ongoing forest expansion. 4370 plots were used in this analysis, removing all plots that coincided with non-forested areas and those not co-located with ALS data. In addition to basic information on forest structure and composition in overstory trees, the inventory also surveys regeneration as well as variables of particular relevance to the management of a national park, such as deadwood amount and quality or specific habitat features (Becker, 2016). In addition to its terrestrial inventory, the national park recently increased its usage of remote sensing data, with a specific focus on ALS (e.g., Senf, Müller and Seidl, 2019; Mandl et al., 2023). BGNP is thus a prime example for considerations of EFI designs because it has a very dense historical inventory grid (that is unlikely to be maintained in its entirety for economic reasons), and because of the availability of remotely sensed data that can be used to aid upcoming inventory cycles. As these conditions are not specific to BGNP but apply to many forest management units across the globe, we perceive the approaches developed herein to be applicable beyond the specific conditions of BGNP.

2.2. Airborne laser scanning data & processing

ALS data were acquired during leaf-on conditions in September 2021 yielding point clouds with an average point density of 47 points m^{-2}. Data were processed using the *lidR* package (v 4.0.2; Roussel et al., 2020) where points were filtered for noise and height normalized. Normalized point clouds were processed to generate wall-to-wall statistical summaries of mean height of points >2 m, canopy cover (percent of points with a height >2 m) and standard deviation of height of points >2 m. These metrics were chosen based on best practice recommendations for including metrics that characterize the height, canopy cover, and variability of forest structure (White et al., 2013). These metrics have also been used extensively within ABA forest attribute modelling due to their often strong relationships with field-measurements (e.g. Næsset, 2004; Woods et al., 2011; Gobakken, Korhonen and Næsset, 2013; Queinnec et al., 2021). These metrics were masked to remove non-forested areas of BGNP, and co-located with terrestrial inventory plots. ALS metrics were extracted for each plot in the systematic sample. The full wall-to-wall coverage of ALS metrics is referred to as the wall-to-wall population for the purposes of comparative statistical analyses.

2.3. Statistical analyses

2.3.1. Monte Carlo sampling simulations

Three Monte Carlo sampling simulations were performed where sample sizes of 20 to 100 in increments of 20, and 100 to 2000 in increments of 50 were iterated 500 times each. The simulations used three sampling methods – Latin hypercube sampling (LHS; Roudier et al., 2012; Ma et al., 2020), spatially balanced sampling through the local pivotal method (LPM; Grafström, Lundström and Schelin, 2012; Grafström and Tillé, 2013), and simple random sampling (SRS; Cochran, 1977). These methods were used to assess potential sampling efficiencies afforded by LHS and LPM over SRS. Individual sampling iterations are referred to as sub-samples to not confuse with the full systematic sample. Sampling was performed using the *sample_existing* algorithm in the *sgsR* package (v1.4.3; Goodbody et al., 2023). Default algorithm parameters were used unless explicitly stated.

2.3.2. Latin hypercube sampling

LHS is a stratified sampling method capable of allocating samples to be representative of underlying multi-dimensional variable distributions (Yang et al., 2020). LHS has been used extensively in environmental science, particularly to model soil attributes (Biswas & Zhang, 2018; Ma et al., 2020; Minasny & McBratney, 2006). Roudier et al. (2012) outline that LHS first divides dimensions of the input feature space into a fixed number of equally sized intervals. These intervals are then randomly sampled to allocate a single point along each dimension. Objective functions are then used to ensure that sampled data and variables are correlated, with iterative improvements performed using a Metropolis-Hastings annealing schedule. This process is repeated until either a stop criterion or a defined number of iterations is reached. A maximum iteration value of 10,000 was used in this study.

2.3.3. Local pivotal method

LPM is a probability-based sampling method first presented by (Deville & Tille, 1998) that allows for unequal probability sampling. Grafström, Lundström and Schelin (2012) adapted this method to provide spatial balance to resulting samples. Grafström and Lundström (2013) highlight that spatially representative samples are balanced – or approximately balanced – with auxiliary variables.

Equal inclusion probabilities for all plots within the systematic sample were used to guide the random selection of a sample unit *i*, following which a nearest neighbour unit *j* is selected based on similarity to all auxiliary variables – ALS metrics in this study. Nearest neighbour selection is the most computationally intensive aspect of the LPM, resulting from the multi-dimensionality of input variables (Lisic & Cruze, 2016). If two or more nearest neighbour units have the same distance to unit *i* then *j* is randomly selected from nearest neighbours. An updating rule function is then applied such that the sampling outcome is decided for one of the two units (*i* or *j*) and inclusion probabilities are updated (Grafström et al., 2012). The unit not selected is considered to be finished (i.e. cannot be chosen again and is no longer considered a neighbour to any other unit). This process is repeated until the desired sample size is reached while ensuring that the sample is spatially representative.

Computationally efficient implementations of LPM are discussed in Grafström et al, (2014) and are presented in the open source R package *BalancedSampling* (Grafström & Lisic, 2018). The simpler and faster local pivotal method 2 implemented using k-d trees (*lpm2_kdtree*) was used for this study. k-d trees are binary trees used to effectively search high dimensional spaces, which is more computationally efficient than linear searches originally used for LPM implementations (Grafström & Lisic, 2018).

2.4. Statistical measures – Parameters & sample statistics

Measures of the mean, variance, as well as 25th and 75th percentiles were calculated for each Monte Carlo sub-sample. The same measures were used to calculate population parameters for the BGNP systematic sample and wall-to-wall ALS metric populations. These measures were chosen to describe central tendency, variability, and percentile ranks of ALS metric distributions. Absolute percent differences (APD) between sub-sample statistics, systematic sample parameters, and wall-to-wall parameters were calculated using:

$$APD_i = \left|\frac{P - s_i}{P}\right| * 100$$

Where P is the parameter measure, s is the sub-sample measure, and i is the Monte Carlo iteration. The average of APD across the 500 Monte Carlo iterations was then calculated to provide the mean absolute percent difference (*MAPD*) The standard deviation of APD was calculated across iterations to provide a measure of dispersion around *MAPD* using:

$$SD_{APD} = \sqrt{\frac{1}{n-1}\sum_{i=1}^{n}(APD_i - MAPD)^2}$$

Where n is the total number of Monte Carlo iterations – 500 for this study. Three independent calculations of *MAPD* were produced. First, sub-sample measures compared with parameters from the full systematic sample ($MAPD_{sys}$), second, sub-sample measures compared with wall-to-wall metric parameters ($MAPD_{w2w}$), and third, wall-to-wall parameters compared with augmented samples allocated using the adapted Latin hypercube evaluation of a legacy sample (AHELS) sampling algorithm described in Section 2.6 ($MAPD_{ahels}$).

2.5. Determination of relative sampling efficiency

A threshold where both *MAPD* and SD_{APD} <5 % was used to identify sub-sample sizes that yielded acceptable levels of precision. The minimum sub-sample size required for LHS and LPM to achieve <5 % thresholds were selected and compared to the minimum equivalent SRS sub-sample size. Relative percent differences between sub-sample sizes for SRS and both LPM and LHS meeting the precision threshold for each ALS metric and statistical measure were calculated as follows, where *rse* is the relative sampling efficiency, x is the sample size for LHS or LPM independently, and y is the sample size for SRS.

$$rse = \left|\frac{x - y}{y} \times 100\right|$$

These relative percent differences in sub-sample size are referred to as relative sampling efficiency (*rse*), indicating the efficiency of LPM and LHS over SRS.

2.6. Adapted Latin hypercube evaluation of a legacy sample

To determine the potential to further reduce $MAPD_{w2w}$ and address any potential systematic bias between sub-sample measures and wall-to-wall ALS parameters, entirely new plot locations from wall-to-wall ALS metric coverages (i.e. not limited to plot locations in the full systematic sample) were added to sub-samples using the AHELS algorithm. Resulting samples include the original sub-sample, as well as newly added plots allocated using AHELS.

The AHELS algorithm was originally described in Malone et al. (2019) to optimize where new plots should be allocated in the context of an existing soil sample. The AHELS algorithm uses an existing sample and auxiliary data – a sub-sample and wall-to-wall ALS metrics in this study – to identify where new plots should be allocated in the distribution of ALS metrics. To do this, the algorithm first stratifies auxiliary metrics into quantiles and generates a density matrix for each. A sampling density matrix is then calculated using the existing sample for the same quantiles. The auxiliary data density and sampling density

matrices are then used to calculate the sampling ratio for each quantile. The sampling ratios are used to determine over- or under-representation within quantiles where a ratio of 1 indicates equal densities. The most under-represented quantiles are preferentially targeted for the allocation of new plots. An iterative sampling approach is employed where new plots are randomly allocated to the quantile with the lowest sampling ratio, which is recalculated each time a plot is added. To control plot allocation, the user can either add a discrete number of plots or set a sampling ratio threshold (e.g. 0.9) beyond which no more plots would be added. The process continues until the specified number of plots or threshold is reached.

The *sample_ahels* function from the *sgsR* package (v1.4.3; Goodbody et al., 2023) was used where Monte Carlo sub-samples were used as existing samples, and the wall-to-wall ALS metrics acted as auxiliary data. The default sampling density threshold of 0.9 was used in place of the addition of a discrete number of plots to allow for an unsupervised optimization of sample size for each existing sub-sample. The number of plots added to each sub-sample using AHELS was recorded to analyze any potential trends.

Following allocation of new plots using AHELS, statistical measures were re-calculated for AHELS augmented sub-samples and $MAPD_{ahels}$ was calculated. $MAPD_{w2w}$ and $MAPD_{ahels}$ were then compared to determine whether the allocation of new plots outside of the systematic sample were capable of improving the precision of sub-sample parameter estimates.

3. Results

3.1. Systematic and wall-to-wall populations

Density distributions of the full systematic sample and wall-to-wall ALS metrics were found to have some disparities (Fig. 2). Lesser regions of canopy cover, mean height and standard deviation of height indicated greater densities in wall-to-wall ALS metrics relative to their full systematic sample equivalents. This likely indicates that the systematic sample is biased towards capturing greater values in chosen ALS metrics.

3.2. Sub-samples vs. full systematic sample

$MAPD_{sys}$ and SD_{sys} were found to be greatest at lesser sample sizes regardless of sampling method, ALS metric, or statistical measure (Fig. 3). $MAPD_{sys}$ and SD_{sys} were consistently greater for SRS than LHS and LPM regardless of sample size. All sampling methods resulted in precise (<5% for $MAPD_{sys}$ and SD_{sys}) estimates of systematic sample parameters, however LHS and LPM were found capable of realizing substantial sampling efficiencies over SRS.

3.3. Sampling efficiencies

Minimum sample sizes required to precisely estimate (<5% for $MAPD_{sys}$ and SD_{sys}) full systematic sample parameters were found to vary depending on the ALS metric and statistical measure being analyzed (Fig. 3). SRS required comparatively larger sample sizes than LHS and LPM to estimate the 25th percentile and variance measures for all ALS metrics. Using SRS, precise estimation of the 25th percentile measure for mean height was found to require the largest sample size of 750, while precise estimation of the same measures for standard deviation of height and canopy cover both required sample sizes of at least 300. A sample size of at least 350 was required for SRS to precisely estimate the variance measure for each ALS metric. LHS realized the greatest sampling efficiency over SRS with 94.3 % (20 vs. 350 plots) for estimating the 25th percentile measure, while LPM realized a maximum increase in efficiency of 88.6 % over SRS (40 vs. 350; Table 1). Precise estimation of the mean measure for all ALS metrics required the lowest sample size tested (20 sample units) for LHS and LPM methods, realizing sampling efficiencies above 65 % compared to SRS. Estimation of the 75th percentile measure was similar, realizing efficiencies over 50 % compared to SRS (Table 1). Estimation of the variance measure for standard deviation of height was the only instance where LPM required a sample size greater than 100 to meet precision thresholds. The maximum sample size required for LHS was 60 plots.

3.4. Sub-samples vs. wall-to-wall metrics

$MAPD_{w2w}$ predominantly resulted in values >5 % precision thresholds (Fig. 4). $MAPD_{w2w}$ was consistently higher than $MAPD_{sys}$ (Fig. 5), indicating potential systematic bias between the ALS metrics co-occurring with the full systematic sample and wall-to-wall ALS structure.

No sampling method for any of the sample sizes tested in this study were capable of precise $MAPD_{w2w}$ values for the 25th percentile measure for any ALS metric. Density distributions indicated differences between lesser values of all ALS metrics between the systematic sample and wall-to-wall ALS metrics, indicating potential reasons why precise $MAPD_{w2w}$ values for the 25th percentile measure were not encountered (Fig. 2). Precise estimates of the 75th percentile measure were achieved for canopy cover and standard deviation of height, with LHS and LPM both realizing sampling efficiencies of 50 % and 67 % over SRS respectively. The mean measure was precisely estimated for standard deviation of

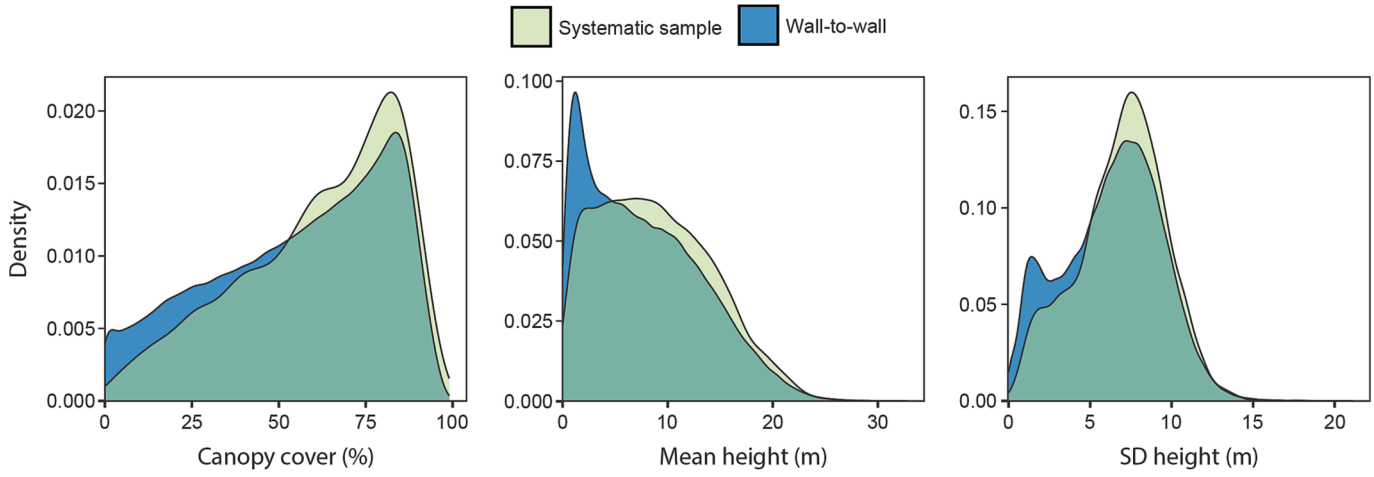

Fig. 2. Density distributions for full systematic sample (green) and wall-to-wall ALS (blue) metrics. (For interpretation of the references to colour in this figure legend, the reader is referred to the web version of this article.)

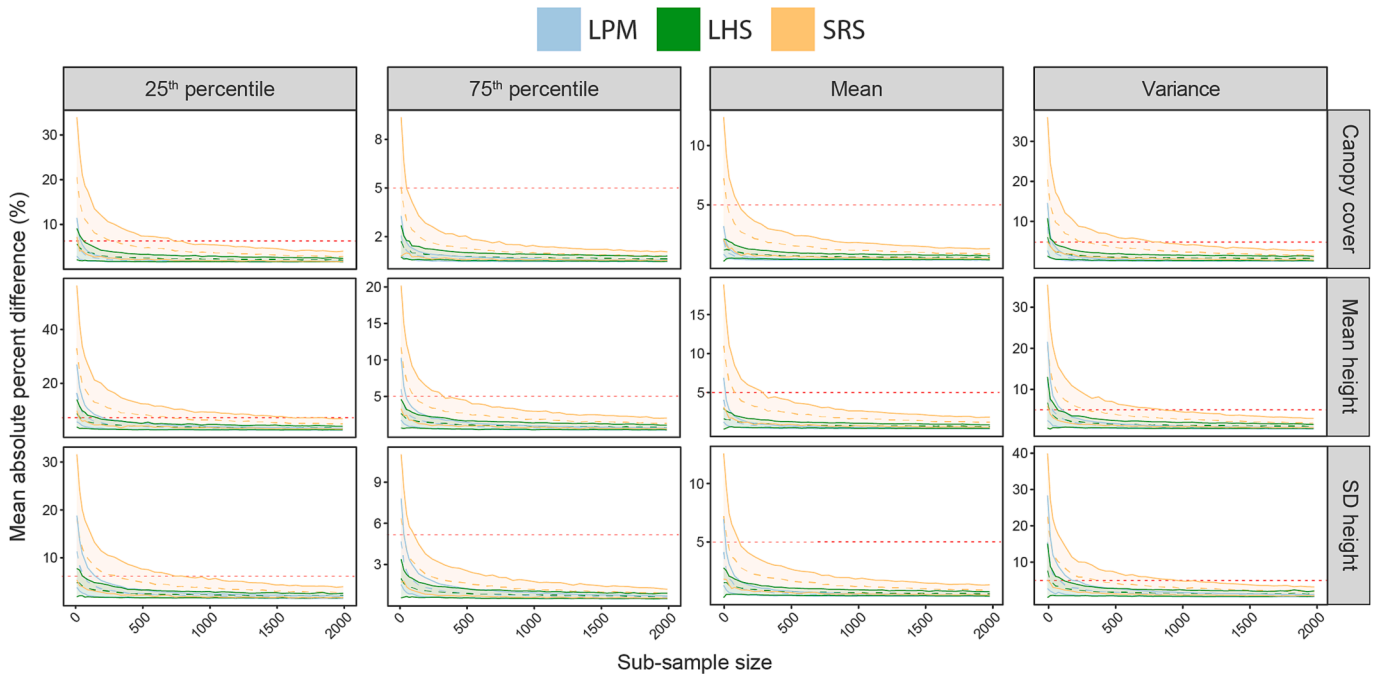

Fig. 3. Mean absolute percent difference ($MAPD_{sys}$) and standard deviation (coloured ribbons) calculated between Monte Carlo sub-sample measures and full systematic sample parameters. Sub-samples were allocated using local pivotal method (LPM; blue), Latin hypercube sampling (LHS; green), and simple random sampling (SRS; orange) methods. The dotted red line indicates the 5% threshold for $MAPD_{sys}$ and SD_{sys}, below which sub-sample sizes were considered precise. (For interpretation of the references to colour in this figure legend, the reader is referred to the web version of this article.)

height with sampling efficiencies of 60 % and 80 % over SRS for LPM and LHS respectively. The variance measure was precisely estimated for mean height and canopy cover, with LHS realizing 89 % and 96 % and LPM realizing 77 % and 92 % over SRS respectively.

3.5. Adapted Latin hypercube evaluation of a legacy sample

Addition of new plots to sub-samples through the application of the AHELS sampling algorithm resulted in $MAPD_{ahels}$ that were substantially reduced compared to $MAPD_{w2w}$ (Fig. 6, Fig. 7). The largest reductions occurred for the 25th percentile measure. Following AHELS sampling, the majority of $MAPD_{ahels}$ values for ALS metrics and measures achieved <5 % MPAD and SD thresholds (Fig. 7). The 25th percentile measure for the mean height metric was the only comparison where the SD threshold was not achieved.

The AHELS sampling density threshold of 0.9 resulted in varying quantities of new plots being allocated to existing sub-samples. Quantity of newly added plots generally decreased from sub-sample sizes of 20 to 200 reaching local minimums (Fig. 8). A linear increase of newly added samples then occurred. This relationship was less pronounced for SRS sub-samples. Interquartile ranges for SRS were consistently greater than those for LPM and LHS. The relationship between decrease in $MAPD_{ahels}$ relative to $MAPD_{w2w}$ indicated that addition of new samples after 250 resulted in diminishing returns (Fig. 7, Fig. 8).

4. Discussion

This study presented objective methods for realizing forest inventory sampling efficiencies. The outcomes of this work could be applied to ecological indicators with direct relationships to ALS-derived vegetation structure. A Monte Carlo sampling simulation was applied where LHS, LPM, and SRS methods were used to sub-sample an existing systematic plot network. The sampling simulation was performed where sub-sample size and sampling method were repeated 500 times each. Sub-sample measures were calculated for each ALS metric and were compared to full systematic sample and wall-to-wall ALS metric parameters. $MAPD_{sys}$ values in our study indicated that sampling efficiencies up to 94.3 % could be realized when using LHS, and up to 88.6 % for LPM relative to SRS. In a simulated sampling study, de Papa et al. (2020) realized sampling efficiencies of up to 41 % over SRS, highlighting that cost savings were enough to offset the acquisition of ALS data, a notable outcome. Confirmation of efficiency gains in this study and in a differing forest type further reinforces the potential for these data-driven sampling approaches to realize considerable financial savings. Mean absolute differences and standard deviations <5 % from systematic sample parameters were achievable through sub-sampling of an existing systematic plot network, with parameters such as the mean and 75th percentile of ALS metrics being achievable with the lowest tested sample size (20 plots). The presented approach is highly flexible, allowing users to alter simulation parameters such as sub-sample sizes, ALS metrics of interest, statistical measures to analyze, and precision thresholds deemed appropriate for management. Resource managers facing budgetary constraints, where only a fraction of an existing sample can be re-measured, could greatly benefit from the approaches presented, providing data driven methods to optimize sample sizes based on statistical similarities between a proposed sample and the underlying ALS metric population.

The secondary objective of this study was to determine whether sub-samples were capable of precisely estimating population parameters for wall-to-wall ALS metrics. $MAPD_{w2w}$ values were markedly higher than $MAPD_{sys}$ for almost all ALS metrics and statistical measures. This indicated that sub-samples – regardless of sampling method – were predominantly not capable of precisely estimating wall-to-wall parameters. ALS metric density distribution comparisons in Fig. 2 and $MAPD_{w2w}$ values for the 25th percentile statistic highlight that lesser values of wall-to-wall metrics were not well captured in the systematic sample. This highlights that using ALS metrics *a priori* could help provide context and confidence that the sample being considered effectively captures variation in the underlying population with known precision. These findings reinforce the efficacy of the LPM (Grafström, Lundström and Schelin, 2012; Grafström and Tillé, 2013), and LHS (Roudier et al., 2012; Ma et al., 2020) sampling approaches and how they are effective

Table 1
Tabular summary of the minimum sample size required to precisely – < 5 % mean absolute percent difference ($MAPD_{sys}$) and standard deviation (SD_{sys}) – estimate systematic sample parameters for ALS metrics. The corresponding required simple random sampling (SRS) sample size equivalent is also presented. Sampling efficiencies (%) of local pivotal method (LPM) and Latin hypercube sampling (LHS) methods over SRS for precisely estimating ALS metric parameters for the full systematic sample.

Sampling method	Statistical measure	ALS metric	Minimum required sample size	SRS equivalent sample size	Efficiency (%) over SRS
LPM	25th percentile	canopy cover	40	300	86.7
		mean height	100	750	86.7
		SD of height	80	350	77.1
	75th percentile	canopy cover	20	40	50.0
		mean height	40	150	73.3
		SD of height	20	40	50.0
	mean	canopy cover	20	60	66.7
		mean height	20	150	86.7
		SD of height	20	60	66.7
	variance	canopy cover	40	350	88.6
		mean height	60	350	82.9
		SD of height	150	400	62.5
LHS	25th percentile	canopy cover	20	300	93.3
		mean height	60	750	92.0
		SD of height	20	350	94.3
	75th percentile	canopy cover	20	40	50.0
		mean height	20	150	86.7
		SD of height	20	40	50.0
	mean	canopy cover	20	60	66.7
		mean height	20	150	86.7
		SD of height	20	60	66.7
	variance	canopy cover	40	350	88.6
		mean height	40	350	88.6
		SD of height	40	400	90.0

for deriving samples that effectively represent the empirical distributions of the underlying population. This serves to also justify application of sample augmentation methods, such as using AHELS, to supplement new plots to improve capturing landscape-level structural heterogeneity.

$MAPD_{w2w}$ values not meeting the <5 % precision thresholds from existing samples raised the need for a data-driven approach to augment the existing sub-sample with newly allocated plots. The AHELS sampling method specifically targeted quantiles where data density and sampling density were unbalanced (Malone et al., 2019), resulting in marked reductions to $MAPD_{ahels}$ relative to $MAPD_{w2w}$ (Fig. 6). In this study we elected to use a sampling density threshold of 0.9 to add plots rather than allocating a discrete number. This facilitated a unsupervised and data-driven allocation of plots to determine whether trends in additional plot quantity would result. Our findings indicated that existing sub-samples with low sample sizes generally required a greater quantity of new plots to be added to reach the 0.9 sampling density threshold. Quantity of newly allocated plots was found to increase linearly with existing sample sizes over sub-sample sizes of approximately 250 plots. This indicates that allocation of new plots at larger sub-sample sizes likely results in small incremental changes to quantile sampling densities, resulting in the need for allocation of larger numbers of plots to reach defined thresholds. The linear increase in newly allocated plots could likely be minimized through the use of a tolerance limit around the desired density threshold (e.g. 0.9±0.05), where the iterative allocation of new plots would ideally allocate samples to the desired density threshold but stop when the tolerance limit is reached. Overall, based on the AHELS precision outcomes, electing to choose a lesser sample size (e.g. 250 plots or less) was most effective from the perspective of cost to statistical precision trade-off, signaling that use of AHELS for larger sample sizes is likely not efficient.

4.1. Management considerations

Improving sampling efficiency using the methods presented in this study could substantially strengthen the ecological indicator domain. Data-driven sampling approaches can result in more precise and accurate indicator estimates (Goodbody et al., 2023), while reductions in bias and uncertainty result in more reliable data that help support creation of robust policy or management plans. Logistical considerations including potential time-savings and cost-reductions could result in plot data being acquired faster with fewer resources, resulting in an overall improvement to deriving meaningful ecological indicators across a land base. Optimizing sample sizes using available remotely sensed data could shift the focus away from logistical challenges associated with field measurement, and instead hone in on which ecological indicators are important for inventories and how to most effectively and comprehensively quantify them.

Important considerations should be applied to the presented results. First and most fundamental is the trade-off between financial cost of sampling and desired precision of estimates. In this study we used a simulation of sub-samples and a precision threshold of <5 % *MAPD* and *SD* to give an example of how a manager may decide to choose an optimal sample size. If financial budgets are constrained, more lenient thresholds for precision may be applied, which would correspondingly influence confidence in estimates. The simulation approach used in this study provided a means to statistically evaluate differences between sub-sample and population measures, and in doing so provided a greater degree of confidence and understanding of risk in selecting a chosen sub-sample size.

Sampling efficiencies over SRS realized in this study indicated that the lowest tested sample size (20 plots) was capable of precisely estimating parameters for the full systematic sample. While these results are interesting in confirming the potential of LHS and LPM sampling methods for estimating population parameters, the effects of using small sample sizes requires critical thought, and there are some caveats to consider with this type of optimized simulation. First, small sample sizes were capable of capturing the mean of the sample but not the variances, confirming that forest practitioners need to consider both mean and variance structures of ALS metrics when designing networks to fully capture landscape variability. Secondly, it is important to note that this analysis did not attempt to incorporate the ability to capture changes in the landscape over time (e.g. Thom & Seidl, 2022). Potential to capture changes would likely require considerably larger sample sizes with a given level of precision. Optimization approaches focused on characterizing change should be pursued.

The selection of a small number of plots reduces potential for statistical replication within an inventory, leading to potential risk. For example, having a single plot to represent a structural stratum in a forest

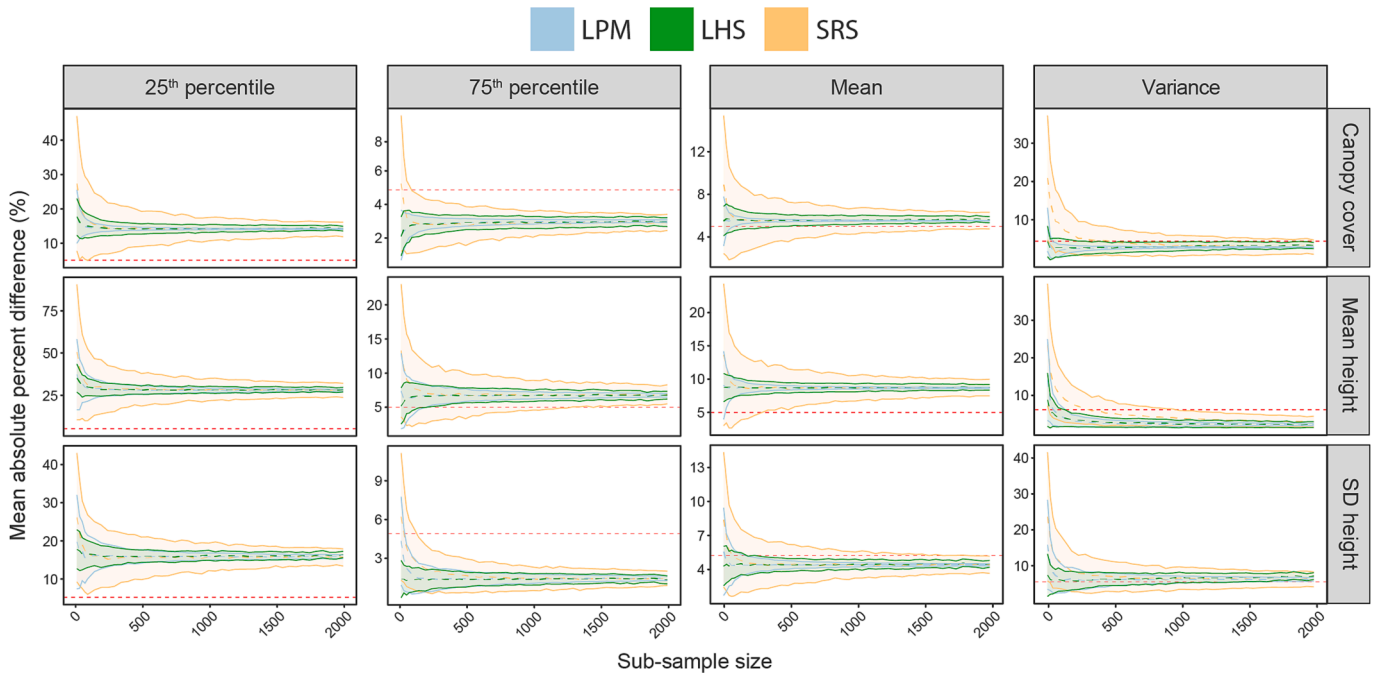

Fig. 4. Mean absolute percent difference ($MAPD_{w2w}$) and standard deviation (coloured ribbons) calculated between Monte Carlo sub-sample measures and wall-to-wall ALS parameters. Sub-samples were allocated using local pivotal method (LPM; blue), Latin hypercube sampling (LHS; green), and simple random sampling (SRS; orange) methods. The dotted red line indicates the 5 % threshold for $MAPD_{w2w}$ and SD_{w2w}, below which sub-sample sizes were considered precise. (For interpretation of the references to colour in this figure legend, the reader is referred to the web version of this article.)

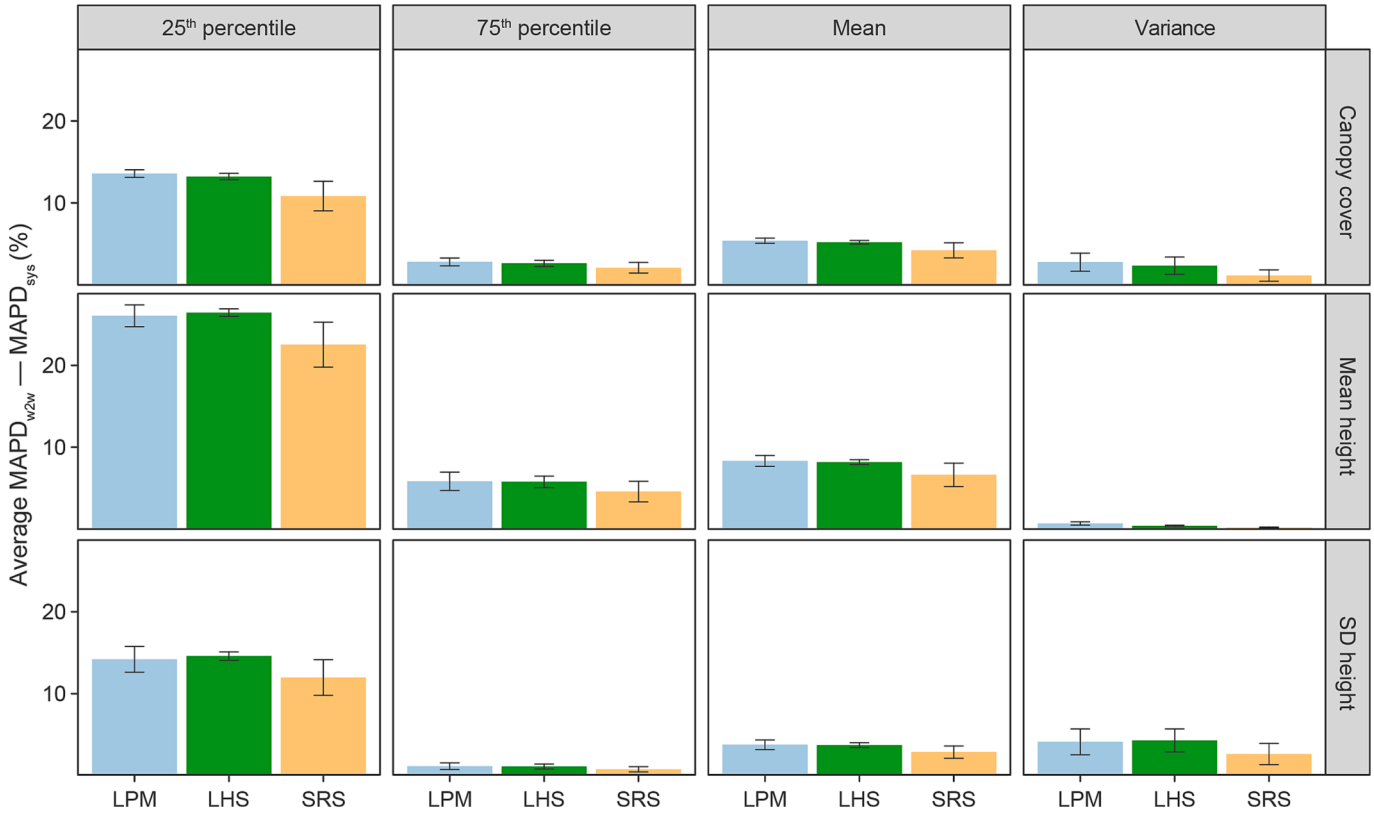

Fig. 5. Average difference between $MAPD_{w2w}$ and $MAPD_{sys}$ for all sampling methods, ALS metrics, and statistical measures. Error bars indicate standard deviation of average differences. Positive values indicate larger values of $MAPD_{w2w}$ compared to $MAPD_{sys}$.

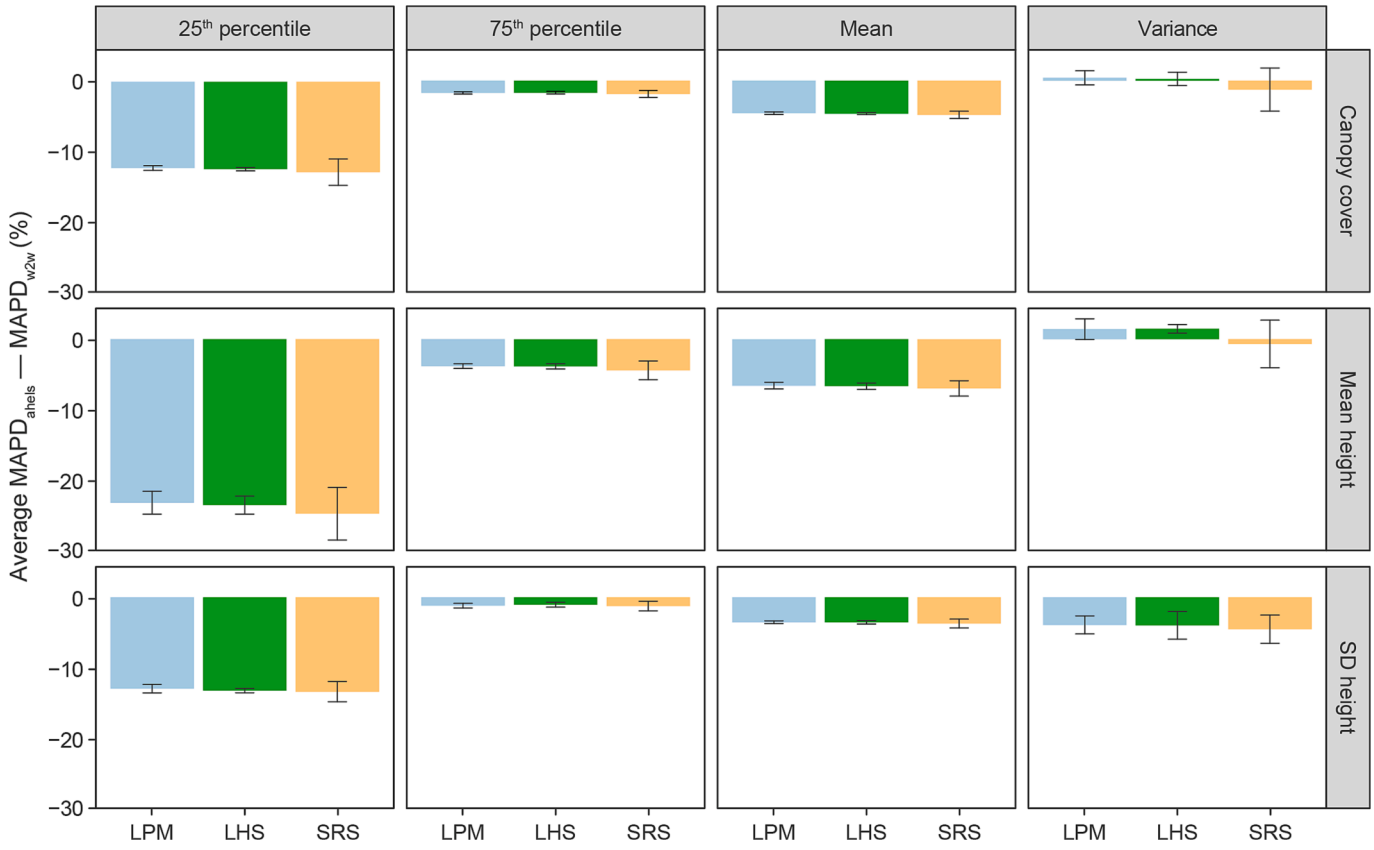

Fig. 6. Average difference between $MAPD_{ahels}$ and $MAPD_{w2w}$ for all sampling methods, ALS metrics, and statistical measures. Error bars indicate standard deviation of average differences. Negative values indicate lesser values of $MAPD_{ahels}$ compared to $MAPD_{w2w}$.

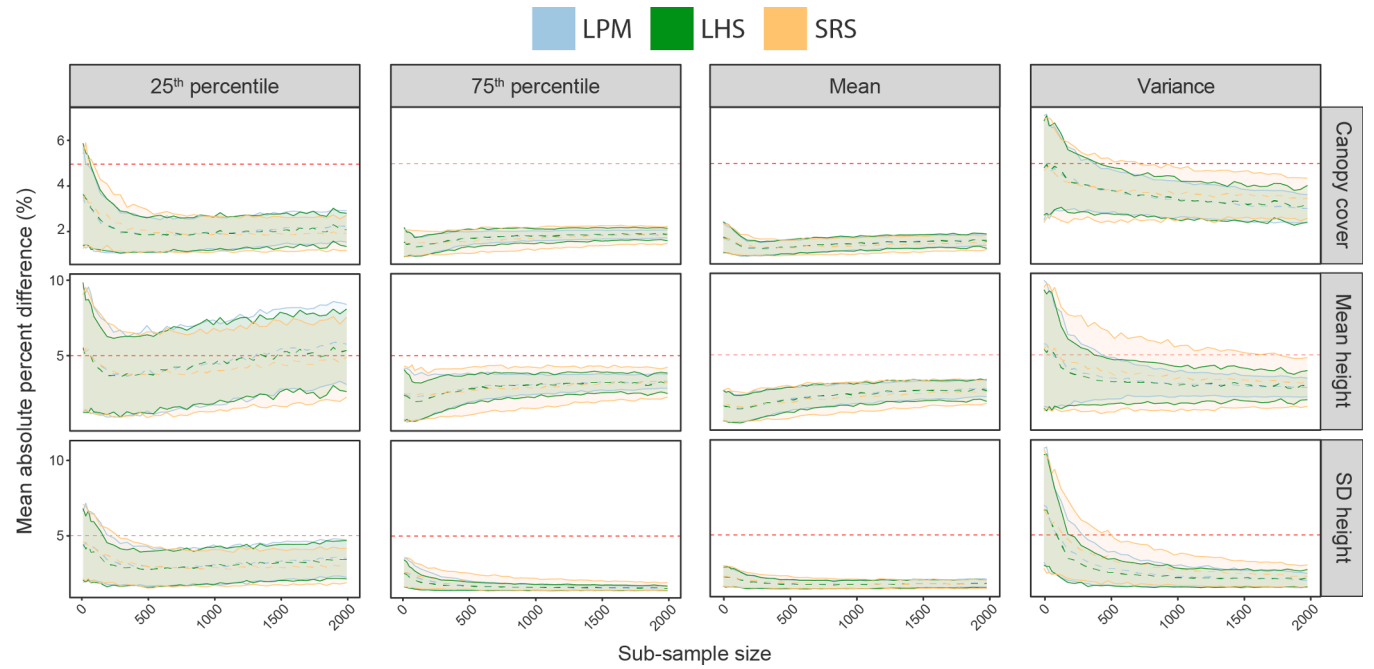

Fig. 7. Mean absolute percent difference ($MAPD_{ahels}$) and standard deviation (coloured ribbons) calculated between Monte Carlo sub-sample measures and wall-to-wall ALS parameters. Sub-samples were allocated using local pivotal method (LPM; blue), Latin hypercube sampling (LHS; green), and simple random sampling (SRS; orange) methods. The dotted red line indicates the 5% threshold for $MAPD_{ahels}$ and SD_{ahels}, below which sub-sample sizes were considered precise. (For interpretation of the references to colour in this figure legend, the reader is referred to the web version of this article.)

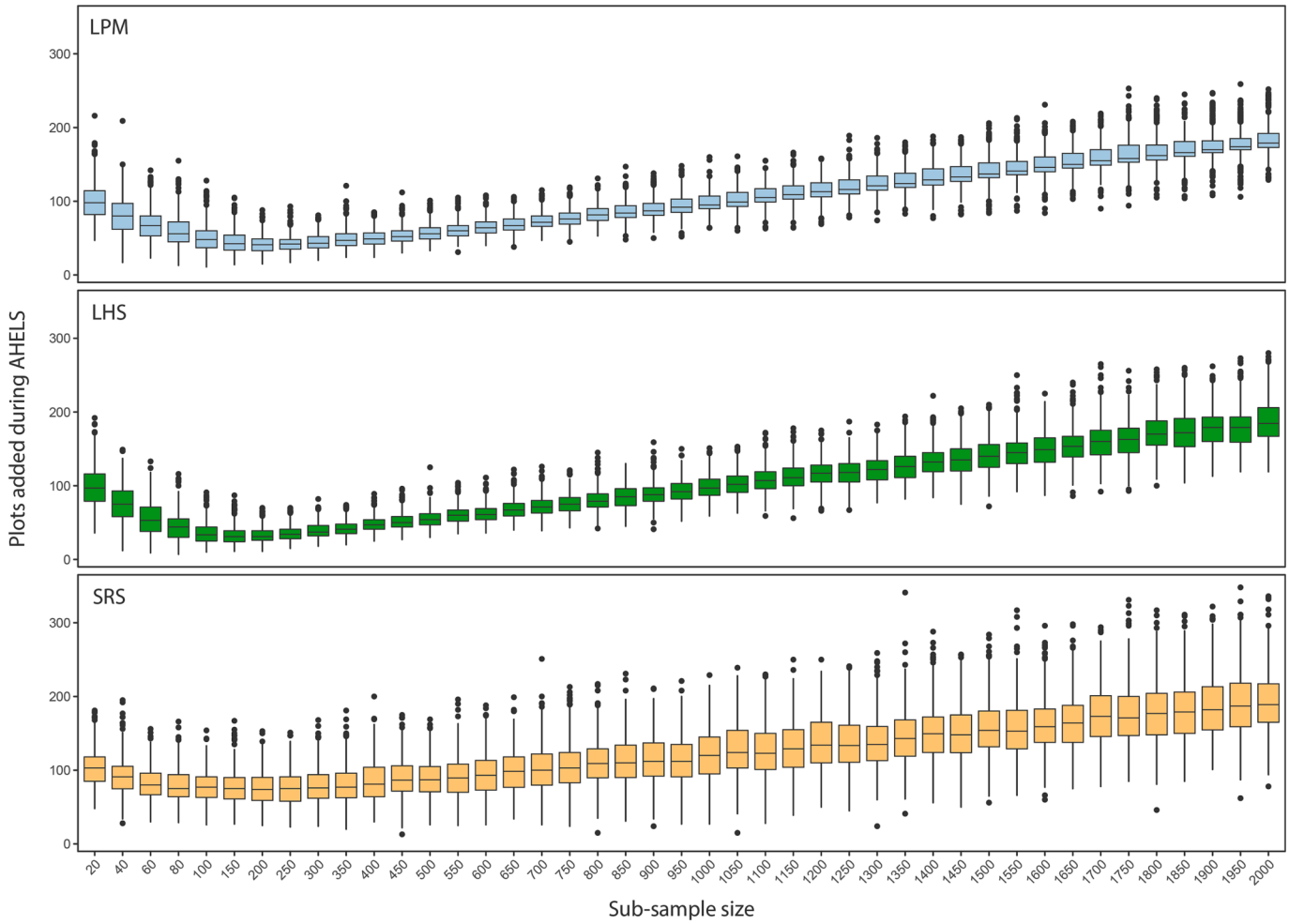

Fig. 8. The number of new plots added using the AHELS sampling method compared to the original sub-sample size for local pivotal method (LPM; blue), Latin hypercube sampling (LHS; green), and simple random sampling (SRS; orange). (For interpretation of the references to colour in this figure legend, the reader is referred to the web version of this article.)

environment may be unwise given local disturbance regimes. Events that impact those specific plot locations are likely to complicate the statistical efficacy of the inventory as a whole. In choosing the minimum possible sample size, practitioners are optimizing the inventory based on the current state of the forest, which could change quickly. For example, BGNP was subject to a large windthrow disturbance event in 2007 which considerably impacted forest structure. Although, redundancy was not incorporated in this studies optimization analysis, it should be an important consideration for forest practitioners to manage risk associated with forest dynamics, especially with ongoing climate change impacts. Additionally, plots replicating structural compositions are an important consideration for research objectives where replication is of considerable importance. As a result, replications of plots within certain strata should be a key consideration when considering these very small optimized sample sizes.

As White et al. (2017) outline, the complexity and variability of a forested environment as well as the intended forest attribute modelling approach should be central to determining an adequate sample size for an inventory. Electing to choose the minimum possible sample size minimizes financial cost of the inventory, but likely introduces undue risk with regards to desired precision of estimates. Unless forest structure across the study area is highly homogenous – the exact opposite of BGNP – the choice in a sample size that appropriately balances the trade off between cost and precision is logical. The potential gradient of precision that is achievable relative to sample size that this study presents should be used as a tool to enable effective decision making relative to logistical constraints. As with many remote sensing derivatives, datasets such as those presented in this study are a tool to facilitate evidence-based management and therefore require thoughtful analysis and consideration. Future research should focus on the potential trade-offs and risks associated with cost and precision. Additionally, studies optimizing the spatial assemblage of plots to both maximize statistical efficacy and minimize field campaign costs should be pursued and supported.

5. Conclusion

Accurate characterization and inventory of forest structure is critical for effectively stewarding forest resources in the face of climate change and increasing financial uncertainty. The trade-off between inventory costs and statistical efficacy do however introduce complexity in deciding on the quantity and location of field plots. The sub-sampling simulations presented in this study present strong evidence that substantial sampling efficiencies can be realized using LHS and LPM over SRS methods. Forest inventories are abundant globally but can similarly be constrained by financial and logistical resources faced at BGNP. Use of ALS as auxiliary information to enhance sampling approaches is well supported by our findings as well as within the context of existing literature. Wall-to-wall structural characterizations afforded by ALS provided opportunity to assess the efficacy of an existing sample network for characterizing landscape level variation and assess probable estimates of precision at varying sample sizes. We outline objective,

simple methods for identifying discrepancies between sample and parameter measures and present approaches to reduce bias and improve precision. We envision that approaches such as these can help practitioners to plan cost-effective and statistically rigorous forest inventory campaigns, especially in the context of where to re-sample in the context of an existing inventory.

Declaration of Competing Interest

The authors declare the following financial interests/personal relationships which may be considered as potential competing interests: Nicholas C. Coops reports financial support was provided by Canadian Wood Fibre Centre.

Data availability

Data will be made available on request.

Acknowledgements

We thank anonymous reviewers and editors for their dedication to improving the relevance of this manuscript.

Funding

This work was supported by the Canadian Wood Fibre Centre's Forest Innovation Program (Project#: AWD-016477), which funded the development of the sgsR package.

References

Aricak, B., Wing, M.G., Akay, A.E., 2022. State of the Art on Airborne LiDAR Applications in the Field of Forest Engineering. In: Suratman, M.N. (Ed.), Concepts and Applications of Remote Sensing in Forestry. Springer Nature, pp. 357–369. https://doi.org/10.1007/978-981-19-4200-6_18.

Ayrey, E., Hayes, D.J., Fraver, S., Kershaw, J.A., Weiskittel, A.R., 2019. Ecologically-Based Metrics for Assessing Structure in Developing Area-Based, Enhanced Forest Inventories from LiDAR. Canadian Journal of Remote Sensing 45 (1), 88–112. https://doi.org/10.1080/07038992.2019.1612738.

Becker, B. (2016). *Der Wald des Alpennationalparks Berchtesgaden. Dritte Waldinventur 2010 – 2012. Forschungsbericht 16, Nationalpark Berchtesgaden.*

Biswas, A., Zhang, Y., 2018. Sampling Designs for Validating Digital Soil Maps: A Review. Pedosphere 28 (1), 1–15. https://doi.org/10.1016/S1002-0160(18)60001-3.

Canadell, J.G., Raupach, M.R., 2008. Managing Forests for Climate Change Mitigation. Science 320 (5882), 1456–1457. https://doi.org/10.1126/science.1155458.

Cochran, W.G., 1977. Sampling techniques. John Wiley & Sons.

Corona, P., Fattorini, L., 2008. Area-based lidar-assisted estimation of forest. Canadian Journal of Forest Research 38 (11), 2911–2916. https://doi.org/10.1139/X08-122.

Papa, D. de A., Almeida, D. R. A. de, Silva, C. A., Figueiredo, E. O., Stark, S. C., Valbuena, R., Rodriguez, L. C. E., & d' Oliveira, M. V. N. (2020). Evaluating tropical forest classification and field sampling stratification from lidar to reduce effort and enable landscape monitoring. *Forest Ecology and Management*, *457*(September 2019). 10.1016/j.foreco.2019.117634.

Deville, J.-C., Tille, Y., 1998. Unequal Probability Sampling Without Replacement Through a Splitting Method. Biometrika 85 (1), 89–101.

Gobakken, T., Korhonen, L., Næsset, E., 2013. Laser-assisted selection of field plots for an area-based forest inventory. Silva Fennica 47 (5), 1–20. https://doi.org/10.14214/sf.943.

Goodbody, T.R.H., Coops, N.C., Queinnec, M., White, J.C., Tompalski, P., Hudak, A.T., Auty, D., Valbuena, R., LeBoeuf, A., Sinclair, I., McCartney, G., Prieur, J.-F., Woods, M.E., 2023. sgsR: a structurally guided sampling toolbox for LiDAR-based forest inventories. Forestry: an International Journal of Forest Research. https://doi.org/10.1093/forestry/cpac055.

Grafström, A., & Lisic, J. (2018). *BalancedSampling: Balanced and Spatially Balanced Sampling* [Computer software]. http://www.antongrafstrom.se/balancedsampling.

Grafström, A., & Lundström, N. L. P. (2013). Why Well Spread Probability Samples Are Balanced. *Open Journal of Statistics*, *3*(1), Article 1. 10.4236/ojs.2013.31005.

Grafström, A., Lundström, N.L.P., Schelin, L., 2012. Spatially Balanced Sampling through the Pivotal Method. Biometrics 68 (2), 514–520. https://doi.org/10.1111/j.1541-0420.2011.01699.x.

Grafström, A., Ringvall, A.H., 2013. Improving forest field inventories by using remote sensing data in novel sampling designs. Canadian Journal of Forest Research 43 (11), 1015–1022. https://doi.org/10.1139/cjfr-2013-0123.

Grafström, A., Saarela, S., Ene, L.T., 2014. Efficient sampling strategies for forest inventories by spreading the sample in auxiliary space. Canadian Journal of Forest Research 44 (10), 1156–1164. https://doi.org/10.1139/cjfr-2014-0202.

Grafström, A., Tillé, Y., 2013. Doubly balanced spatial sampling with spreading and restitution of auxiliary totals. Environmetrics 24 (2), 120–131. https://doi.org/10.1002/env.2194.

Hawryło, P., Tompalski, P., Wężyk, P., Węzyk, P., 2017. Area-based estimation of growing stock volume in Scots pine stands using ALS and airborne image-based point clouds. Forestry 90 (5), 686–696. https://doi.org/10.1093/forestry/cpx026.

Iqbal, I.A., Musk, R.A., Osborn, J., Stone, C., Lucieer, A., 2019. A comparison of area-based forest attributes derived from airborne laser scanner, small-format and medium-format digital aerial photography. International Journal of Applied Earth Observation and Geoinformation 76 (December 2018), 231–241. https://doi.org/10.1016/j.jag.2018.12.002.

Junttila, V., Finley, A.O., Bradford, J.B., Kauranne, T., 2013. Strategies for minimizing sample size for use in airborne LiDAR-based forest inventory. Forest Ecology and Management 292, 75–85. https://doi.org/10.1016/j.foreco.2012.12.019.

Kangas, A., Astrup, R., Breidenbach, J., Fridman, J., Gobakken, T., Korhonen, K.T., Maltamo, M., Nilsson, M., Nord-Larsen, T., Næsset, E., Olsson, H., 2018. Remote sensing and forest inventories in Nordic countries – roadmap for the future. Scandinavian Journal of Forest Research 33 (4), 397–412. https://doi.org/10.1080/02827581.2017.1416666.

Kurniawan, R., Managi, S., 2018. Economic Growth and Sustainable Development in Indonesia: An Assessment. Bulletin of Indonesian Economic Studies 54 (3), 339–361. https://doi.org/10.1080/00074918.2018.1450962.

Lisic, J. J., & Cruze, N. B. (2016). *Local Pivotal Methods for Large Surveys*.

Ma, T., Brus, D.J., Zhu, A., Zhang, L., Scholten, T., 2020. Comparison of conditioned Latin hypercube and feature space coverage sampling for predicting soil classes using simulation from soil maps. Geoderma 370 (April), 114366. https://doi.org/10.1016/j.geoderma.2020.114366.

Malone, B.P., Minansy, B., Brungard, C., 2019. Some methods to improve the utility of conditioned Latin hypercube sampling. PeerJ 7, e6451.

Maltamo, M., Packalen, P., Kangas, A., 2021. From comprehensive field inventories to remotely sensed wall-to-wall stand attribute data-a brief history of management inventories in the nordic countries. Canadian Journal of Forest Research 51 (2), 257–266. https://doi.org/10.1139/cjfr-2020-0322.

Mandl, L., Stritih, A., Seidl, R., Ginzler, C., & Senf, C. (2023). Spaceborne LiDAR for characterizing forest structure across scales in the European Alps. *Remote Sensing in Ecology and Conservation*, *n/a*(n/a). 10.1002/rse2.330.

Melville, G., Stone, C., Turner, R., 2015. Application of LiDAR data to maximise the efficiency of inventory plots in softwood plantations. New Zealand Journal of Forestry Science 45 (1), 9. https://doi.org/10.1186/s40490-015-0038-7.

Minasny, B., McBratney, A.B., 2006. A conditioned Latin hypercube method for sampling in the presence of ancillary information. Computers & Geosciences 32 (9), 1378–1388. https://doi.org/10.1016/j.cageo.2005.12.009.

Næsset, E., 2004. Accuracy of forest inventory using airborne laser scanning: Evaluating the first Nordic full-scale operational project. Scandinavian Journal of Forest Research 19 (6), 554–557. https://doi.org/10.1080/02827580410019544.

Næsset, E., 2015. Area-based inventory in Norway – from innovations to operational reality. In: Maltamo, M., Næsset, E., Vauhkonen, J. (Eds.), Forestry Applications of Airborne Laser Scanning. Springer, Concepts and Case Studies.

Queinnec, M., Coops, N.C., White, J.C., McCartney, G., Sinclair, I., 2021. Developing a forest inventory approach using airborne single photon lidar data: From ground plot selection to forest attribute prediction. Forestry: an International Journal of Forest Research 1–16.

Roudier, P., Hewitt, A. E., & Beaudette, D. E. (2012). A conditioned Latin hypercube sampling algorithm incorporating operational constraints. *Digital Soil Assessments and Beyond – Proceedings of the Fifth Global Workshop on Digital Soil Mapping*, 227–231. 10.1201/b12728-46.

Roussel, J.-R., Auty, D., Coops, N.C., Tompalski, P., Goodbody, T.R.H., Meador, A.S., Bourdon, J.-F., de Boissieu, F., Achim, A., 2020. lidR: An R package for analysis of Airborne Laser Scanning (ALS) data. Remote Sensing of Environment 251 (August), 112061. https://doi.org/10.1016/j.rse.2020.112061.

Senf, C., Seidl, R., Hostert, P., 2017. Remote sensing of forest insect disturbances: Current state and future directions. International Journal of Applied Earth Observation and Geoinformation 60, 49–60. https://doi.org/10.1016/j.jag.2017.04.004.

Senf, C., Müller, J., Seidl, R., 2019. Post-disturbance recovery of forest cover and tree height differ with management in Central Europe. Landscape Ecology 34 (12), 2837–2850. https://doi.org/10.1007/s10980-019-00921-9.

Swamy, L., Drazen, E., Johnson, W.R., Bukoski, J.J., 2018. The future of tropical forests under the United Nations Sustainable Development Goals. Journal of Sustainable Forestry 37 (2), 221–256. https://doi.org/10.1080/10549811.2017.1416477.

Thom, D., Seidl, R., 2022. Accelerating Mountain Forest Dynamics in the Alps. Ecosystems 25 (3), 603–617. https://doi.org/10.1007/s10021-021-00674-0.

Tompalski, P., Coops, N.C., White, J.C., Wulder, M.A., 2015. Enriching ALS-derived area-based estimates of volume through tree-level downscaling. Forests 6 (8), 2608–2630. https://doi.org/10.3390/f6082608.

Tompalski, P., Coops, N.C., Wulder, M.A., Bailey, T., 2018. Combining Multi-Date Airborne Laser Scanning and Digital Aerial Photogrammetric Data for Forest Growth and Yield Modelling. Remote Sensing 10 (2), 1–21. https://doi.org/10.3390/rs10020347.

Tomppo, E., Gschwantner, T., Lawrence, M., McRoberts, R.E., 2010. National Forest Inventories Pathways for Common Reporting. Springer, Netherlands. https://doi.org/10.1007/978-90-481-3233-1.

Verkerk, P.J., 2022. Forest products in the global bioeconomy: Enabling substitution by wood-based products and contributing to the Sustainable Development Goals. FAO. https://doi.org/10.4060/cb7274en.

White, J.C., Wulder, M.A., Varhola, A., Vastaranta, M., Coops, N.C., Cook, B.D., Pitt, D., Woods, M., 2013. A best practices guide for generating forest inventory attributes

from airborne laser scanning data using an area-based approach. The Forestry Chronicle 89 (06), 722–723. https://doi.org/10.5558/tfc2013-132.

White, J.C., Coops, N.C., Wulder, M.A., Vastaranta, M., Hilker, T., Tompalski, P., 2016. Remote Sensing Technologies for Enhancing Forest Inventories: A Review. Canadian Journal of Remote Sensing 42 (5), 619–641. https://doi.org/10.1080/07038992.2016.1207484.

White, J.C., Tompalski, P., Vastaranta, M., Wulder, M.A., Saarinen, N., Stepper, C., Coops, N.C., 2017. A model development and application guide for generating an enhanced forest inventory using airborne laser scanning data and an area-based approach. Canadian Forest Service, Canadian Wood Fibre Centre, Pacific Forestry Centre, pp. 1–48.

Woods, M., Pitt, D., Penner, M., Lim, K., Nesbitt, D., Etheridge, D., Treitz, P., 2011. Operational implementation of a LiDAR inventory in Boreal Ontario. The Forestry Chronicle 87 (04), 512–528. https://doi.org/10.5558/tfc2011-050.

Yang, L., Li, X., Shi, J., Shen, F., Qi, F., Gao, B., Chen, Z., Zhu, A.X., Zhou, C., 2020. Evaluation of conditioned Latin hypercube sampling for soil mapping based on a machine learning method. Geoderma 369 (October 2019), 114337. https://doi.org/10.1016/j.geoderma.2020.114337.